

Analysis of Annual Rainfall Climate Variability in Saudi Arabia by Using Spectral Density Function

Amro Elfeki, Nassir Al-Amri and Jarbou Bahrawi

Department of Hydrology and Water Resources Management,
Faculty of Meteorology, Environment and Arid Land Agriculture,
King Abdulaziz University, P.O. Box: 80208 Jeddah 21589 Saudi Arabia

Abstract: Climate variability is becoming a fact; many locations in the world are suffering from either extreme floods or extreme droughts. Nowadays engineers and scientists are exploring tools to analyze this variability and try to quantify it and include in climate models in order to improve model predictions. In this paper, a spectral density function (SDF) approach is going to be utilized to analysis annual rainfall signals in the south western part of the Kingdom of Saudi Arabia. Through the SDF approach the climate cycles has been inferred from the data. Some longest annual rainfall stations (7 stations) with records between 42 years to 50 years are analyzed. Results show multiple cyclic components with significant variances. The common cycle for the seven stations has a period of 26 years (almost quarter of a century). This cycle has the strongest impact on rainfall climate variability for almost all stations in comparison with other cycles.

Key words: Annual rainfall, Arid zones, Climate variability, Saudi Arabia and Spectral density function

INTRODUCTION

Climate variability is one of the hot issues word wide. Some researchers believe that increasing environmental population and accelerating economic development activities are the cause of such variability. However, others believe that this variability is a natural cycle of the earth's climate. There is a lot of debate between those two parties. The consequences of climate variability can be manifested in the higher frequency of extremes such as floods and droughts. Floods are associated with extremes in rainfall from tropical storms, thunderstorms, orographic rainfall, widespread extratropical cyclones, etc., while droughts are associated with the lack of precipitation and often extreme high temperatures that contribute to drying. Floods are often fairly local and develop on short timescales, while droughts are extensive and develop over months or years.

Rodriguez-Puela *et al.* [1] have studied spatial and temporal pattern of the annual precipitation variability over the Iberian Peninsula. They used 17 stations distributed over the peninsula with precipitation records

of 47 years. They were concerned particularly with the threat of desertification throughout the Iberian Peninsula. They used the spectral analysis together with principle component approach (PC) in order to obtain the structure of the temporal variations. The spectra of the precipitation show statistically significant oscillations. The most significant oscillations are: 3-6 years for PC1; 6-9 years for PC2; 16 years and 2-3 years for PC3; 6-9 years for PC4.

In this paper, the authors investigated the rainiest part in the Kingdom of Saudi Arabia which is the south western part. The stations considered in this analysis are seven stations namely A121, B101, J102, J113, SA104, SA110 and SA111. Table 1 shows the geographic locations of these stations, the elevation of the station and the period of records. The elevations vary from stations near the red sea with elevation of 116 m, up to stations on high mountains of elevations of about 2330 m. The station records vary between 42 years for station A121 up to 50 years at station B101. Figure 1 shows the geographic locations of the stations consider in the analysis, while, Figure 2 shows the annual time series of a sample station (A121) where one can observe

Corresponding Author: Amro Elfeki, Department of Hydrology and Water Resources Management,
Faculty of Meteorology, Environment and Arid Land Agriculture,
King Abdulaziz University, P.O. Box: 80208 Jeddah 21589 Saudi Arabia

Table 1: Stations considered in the analysis.

Station Name	Station Code	Coordinates		Elevation (m)	Records Period	
		North	East		From	To
TEMNIYAH	A121	18.03	42.75	2300	1965	2006
AJAEDA	B101	19.90	41.58	2330	1960	2011
BAHRAH	J102	21.43	39.70	116	1966	2011
FARRAIN	J113	21.37	40.12	520	1966	2005
ARDAH	SA104	17.05	43.08	223	1960	2006
JABAL FAYFA	SA110	17.27	43.13	860	1960	2006
JABAL SALA	SA111	17.05	43.12	900	1960	2006

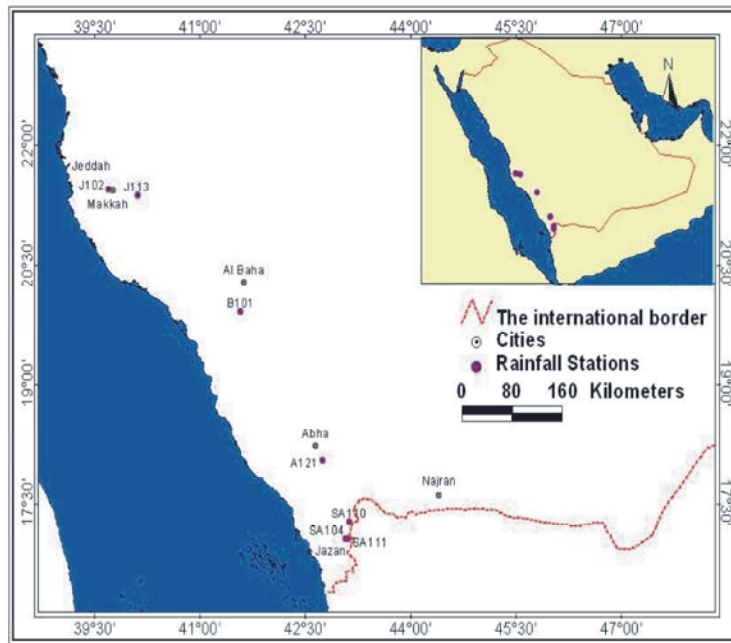


Fig. 1: Spatial distribution of the stations considered in the analysis

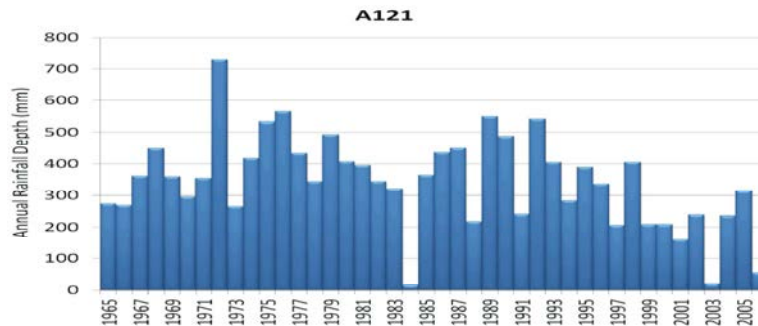


Fig. 2: Sample annual time series of one of the stations (Station A121)

the maximum rainfall is 729 mm occurred on 1972 (wet year) and the minimum rainfall is 16 mm occurred on 1984 (dry year). The annual average rainfall of such station is 342 mm and the stander deviation is 144 mm and the coefficient of variation is about 0.42 showing relatively low variability around the mean.

MATERIALS AND METHODS

In the current study, the theory of stochastic processes [2] has been adopted to analyze the annual rainfall signals. The theory of stochastic processes is mainly based on the autocorrelation function and power

spectral density functions. In the coming sections, an explanation of these tools for the analysis of rainfall signals.

Autocorrelation Function: Properties of stationary stochastic process $Z(t)$ may be represented in a time domain which is represented by the autocorrelation function of the lag τ . The autocorrelation function, ρ_{ZZ} , is expressed as [3].

$$\rho_{ZZ}(\tau) = \frac{\text{Cov}(Z(t+\tau), Z(t))}{\sigma_z^2} \quad (1)$$

where, $Z(t)$ and $Z(t+\tau)$ are the stochastic process at two locations separated by a lag τ ,

σ_z^2 is the variance of the stochastic process and $\text{Cov}(Z(t+\tau), Z(t))$ is the covariance of the stochastic process at lag τ , which is given by,

$$\text{Cov}(Z(t+\tau), Z(t)) = \frac{1}{n(\tau)} \sum_{j=1}^{n(\tau)} [Z(t_j+\tau) - \bar{Z}][Z(t_j) - \bar{Z}] \quad (2)$$

where, $n(\tau)$ is the number of points with separation lag τ . The graph that represents correlation coefficients between values of the process versus the lag τ is called the correlogram.

The auto-correlation function has the following properties,

$$\begin{aligned} \rho_{ZZ}(0) &= 1 \\ \rho_{ZZ}(\infty) &= 0 \\ \rho_{ZZ}(\tau) &= \rho_{ZZ}(-\tau) \end{aligned} \quad (3)$$

The Power Spectral Density Function: The term power is commonly seen in the literature. Its origin comes from the field of electrical and communication engineering: power dissipated in an electrical circuit is proportional to the

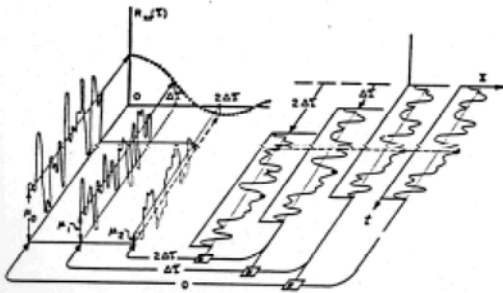


Fig. 3: Correlogram: graphical representation of correlogram calculation (note that the $X(t)$ in the graph correspond to $Z(t)$ in the equations and $R_{xx}(\tau)$ corresponds to $C_{zz}(\tau)$)

mean square voltage applied. The adjective spectral denotes a function of frequency. The concept of density comes from the division of the power (variance) of an infinitesimal frequency interval by the width of that interval. The power spectrum describes the distribution of power (variance) with frequency of the random processes and as such is real and non-negative [4].

The auto-power spectrum, $S_{zz}(f)$, (spectral density function) for a process $Z(t)$ is given by;

$$S_{zz}(f) = \lim_{L \rightarrow \infty} \frac{1}{L} \overline{[z(f) \cdot z^*(f)]} = \lim_{L \rightarrow \infty} \frac{1}{L} \overline{|z(f)|^2} \quad (4)$$

where, L is the length of the signal in the frequency domain, the over bar means a sample time average and $z(f)$ is Fourier transform of the process $Z(t)$, which is expressed as;

$$z(f) = \frac{1}{2\pi} \int_{-\infty}^{\infty} Z(t) e^{-i2\pi ft} dt \quad (5)$$

and $z^*(f)$ is the conjugate of $z(f)$ and f is the angular frequency.

Properties of the Auto-power spectrum are formulated as;

$$\begin{aligned} S_{zz}(f) &\geq 0 \\ \int_{-\infty}^{\infty} S_{zz}(f) df &= \sigma_z^2 \\ S_{zz}(f) &= S_{zz}(-f) \end{aligned} \quad (6)$$

The covariance functions and spectral density functions are Fourier transform pairs. This can be expressed in mathematical forms using Wiener-Khinchin relationships given by [5];

$$\begin{aligned} S_{zz}(f) &= \frac{1}{2\pi} \int_{-\infty}^{\infty} C_{zz}(\tau) e^{-i2\pi f\tau} d\tau \\ C_{zz}(\tau) &= \int_{-\infty}^{\infty} S_{zz}(f) e^{i2\pi f\tau} df \\ C_{zz}(0) &= \int_{-\infty}^{\infty} S_{zz}(f) df = \sigma_z^2 \end{aligned} \quad (7)$$

Since the auto-power spectrum is an even function, therefore the formula can be re-casted as;

$$S_{zz}(f) = \frac{1}{\pi} \int_0^{\infty} C_{zz}(\tau) \cos(2\pi f\tau) d\tau \quad (8)$$

The above equation can be formulated numerically using the trapezoidal rule of integration as,

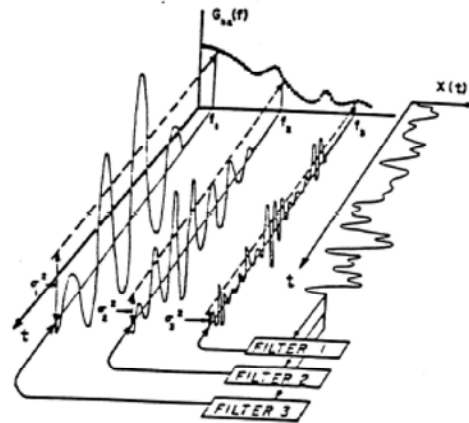


Fig. 4: Periodogram: graphical representation of periodogram calculations (note that the $X(t)$ in the graph correspond to $Z(t)$ in the equations and $G_{xx}(f)$ corresponds to $S_{zz}(f)$)

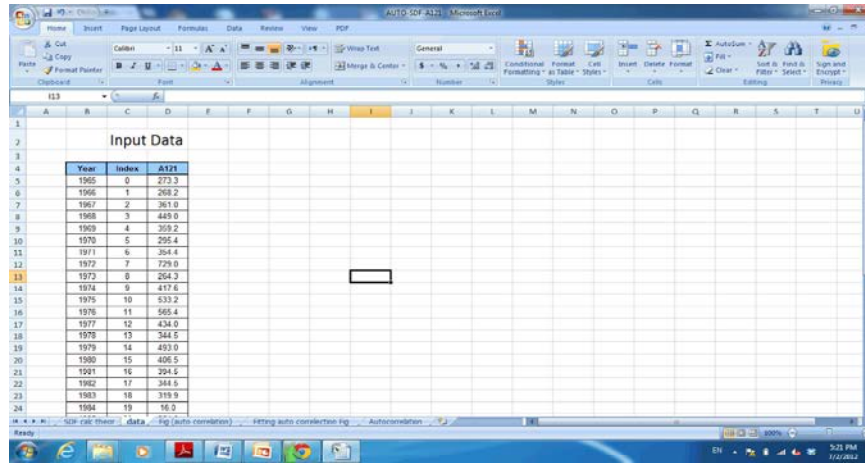


Fig. 5: Input data sheet

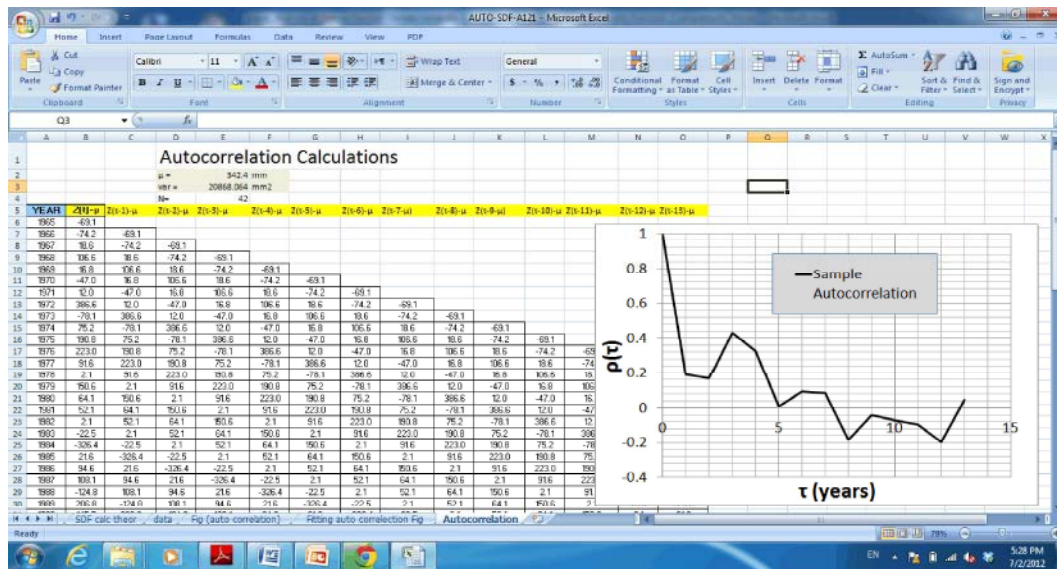


Fig. 6: Calculation of autocorrelation function sheet

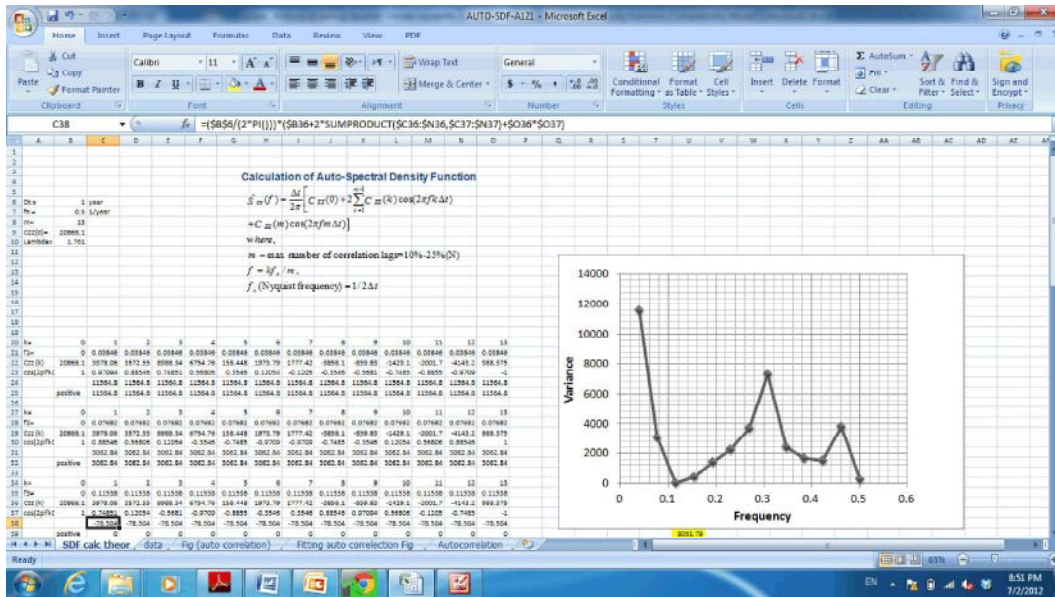


Fig. 7: Calculation of spectral density function sheet

$$\hat{S}_{zz}(f) = \frac{\Delta t}{2\pi} \left[C_{zz}(0) + 2 \sum_{k=1}^{m-1} C_{zz}(k) \cos(2\pi f k \Delta t) + C_{zz}(m) \cos(2\pi f m \Delta t) \right] \quad (10)$$

where,

$$f = k f_n / m,$$

$$f_n \text{ (Nyquist frequency)} = 1/2\Delta t$$

$$k = 0, 1, 2, \dots, m$$

A spreadsheet model has been developed to perform such calculation. The model is simple in the sense that the rainfall data is inserted in the first sheet and the model automatically performs the rest of the calculations based on the spreadsheet built in functions and authors-made calculations. The following figures show some of the model windows. Figure 5 shows the input data sheet, where it contains the annual rainfall time series. Figure 6 reads the input data and calculates the correlation function by shifting the input signal by one year and put them in another column and the correlation coefficient between the two signals is calculated. This process is repeated by shifting the signal more cells and each time the correlation coefficient is calculated between the original signal and the signal after shifting to calculate the autocorrelation function as a function of the shifting lag (correlogram), as presented in Figure 7. Figure 8 shows the sheet designed for the calculation of the variance spectrum (or periodogram). The sheets calculated the numerical integration given in Equation 10.

RESULTS AND DISCUSSION

In this section, the analysis of the results has been made. The time-scale variability of the rainfall signals has been obtained using spectral analysis explained in the aforementioned section based on Blackman and Tukey procedure to compute the spectrum, which is also based on the Fourier transform of the serial correlation coefficients with a consistent estimate of the spectrum [6]. Time series consist of an infinite number of oscillations and the spectral analysis, with the stationary assumption, distributes the variance from the lowest to the Nyquist frequencies [7].

Table 2 shows the summary statistics of the analysis. It has been shown that the integral time scale is between 0.7 to 1.8 years, which is an indication of very short correlation time scale in the rainfall time series. The lag⁻¹ autocorrelation (ρ_1) do not show evidence of a significant persistence (average $\rho_1=0.13$), with exception for station SA 110 that shows relatively higher persistence of about 0.56. Figures 9 to 11 show the autocorrelation function calculated from the rainfall data for thirteen lags and the corresponding spectral density function. The figures show that the autocorrelation different patterns. Stations J102 and J113 show short range correlation where the autocorrelation between lag-0 to lag-1 drops significantly. The integral scale of the two stations is less than one year as indicated

Table 2: Statistical Parameters of the Stations.

Station Name	Station Code	Statistical Parameters		Integral Scale (Years)	Lag 1 Auto correlation	Period of Peak Variance (Years)
		Annual Mean (mm)	Annual Variance (mm ²)			
TEMNIYAH	A121	342	20868	1.8	0.19	26, 3.25, 2.1
AJAEDA	B101	216	23722	1.3	0.26	26, 3.25, 2.6, 2
BAHRAH	J102	45	2124	0.7	0.10	26, 4.3, 2
FARRAIN	J113	139	8254	0.9	-0.12	26, 3.25, 2
ARDAH	SA104	445	43482	1.5	0.24	26, 8.7, 3.7, 2.6
JABAL FAYFA	SA110	379	76049	1.3	0.56	26, 13, 6.5
JABAL SALA	SA111	498	276907	1.3	0.11	26, 3.7, 2.2

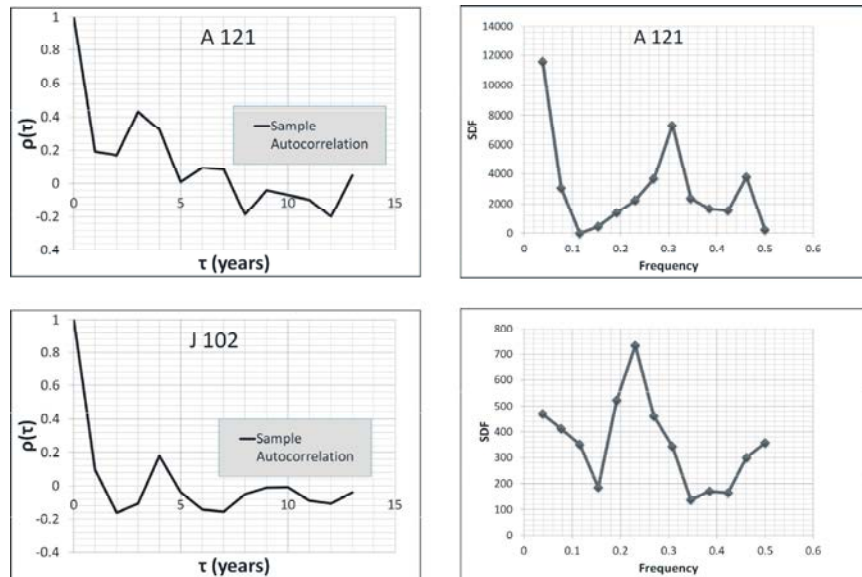


Fig. 8: Auto-correlation function and the corresponding spectral density function of the rainfall data at stations A121 and J02

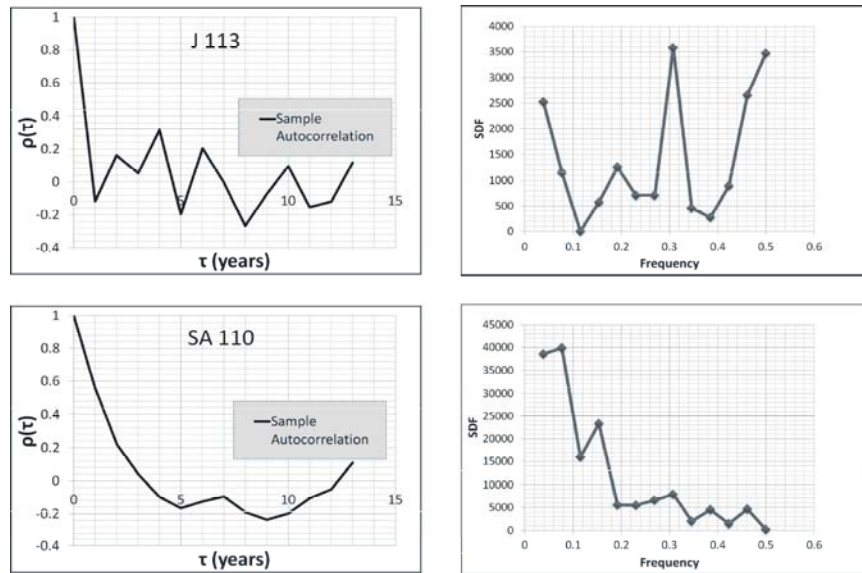


Fig. 9: Auto-correlation function and the corresponding spectral density function of the rainfall data at stations J113 and SA110

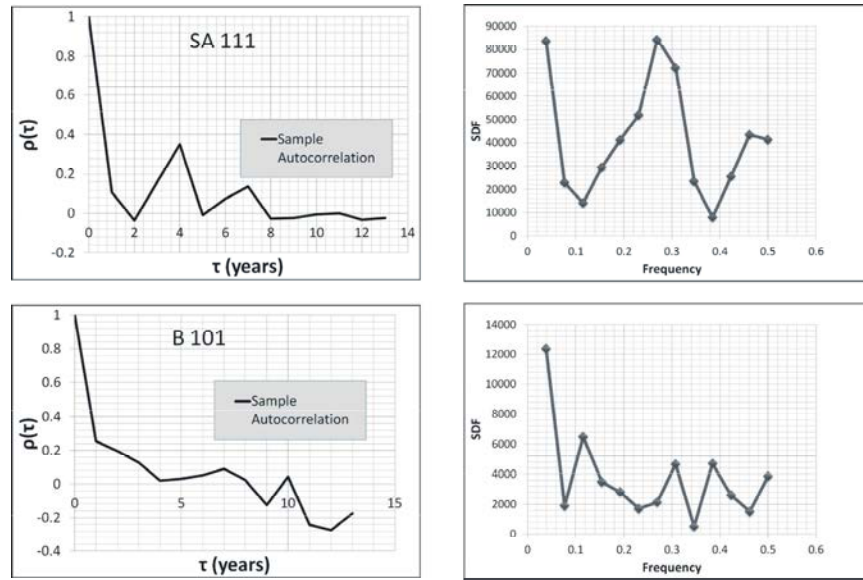


Fig. 10: Auto-correlation function and the corresponding spectral density function of the rainfall data at stations SA111 and B101

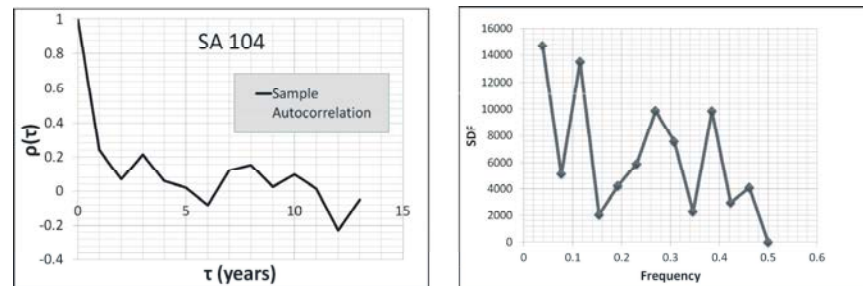


Fig. 11: Auto-correlation function and the corresponding spectral density function of the rainfall data at station SA104

by Table 2. However, for stations A121, SA110, SA111, SA104 and B101 the figures show relatively longer autocorrelation. The corresponding integral scale is larger than 1 year as indicated in Table 2.

The spectral density functions represented graphically in Figures 9 to 11 show different periodicity of the significant variance. The common periodicity is 26 years which is available in all stations, however, for stations A121, B101 and J113 there is a significant variance with oscillation of 3.25 years. Stations A121, B101, J102, J113, SA 111 shows oscillations of a period of 2 years on average. There is also a unique oscillation for station SA 104 of a period of 8.7 years and SA 110 of a period of 13 years and 6.5 years. The analysis shows multiple temporal scales were obtained with relatively significant variance and it is therefore difficult to identify the organized structures in the spectra from all stations except the 26 years cycle that is common in all stations.

One could extract the average significant oscillations from all stations to be 26, 13, 6.5, 3.5 and 2 years.

CONCLUSIONS

In this study we have documented information on the temporal structures of annual precipitation over the south western part of Saudi Arabia. Autocorrelation and spectral analysis methods were used to examine the modes of variation. The following conclusions are obtained. When spectral analysis is applied to the local precipitation time series, multiple temporal scales were obtained with relatively significant variance and it is therefore difficult to identify the organized structures in the spectra except that the 26 years cycle is common for all stations. However, one could extract the average significant cycles from all stations to be 26, 13, 6.5, 3.5 and 2 years.

One of the applications of this study is the possibility for building time series models from the available data. The models are based on the reconstruction of the significant 'signals' from the data.

ACKNOWLEDGMENT

The authors would like to thank Mr. Abdelaziz Al-Bishri for some data preparation and GIS map of the stations.

REFERENCES

1. Rodriguez-Puela, C., A.H. Encinas, S. Nieto and J. Garmendia, 1998. Spatial and temporal pattern of annual precipitation variability over the Iberian Peninsula. *Int. J. Climatol.*, 18: 299-316.
2. Yevjevich, V., 1972. *Stochastic Processes in Hydrology*, Water Resources Publications. Fort Collins, Colorado, USA.
3. Bras, R.L. and I. Rodriguez-Iturbe, 1984. *Random functions and hydrology*. Addison-Wesley Publishing Company, Inc.
4. Vanmarcke, E., 1983. *Random Fields: Analysis and Synthesis*, Cambridge, Mass: MIT Press.
5. Kay, S.M., 1988. *Modern Spectral Estimation*. Prentice Hall.
6. Brockwell, P.J. and R.A. Davis, 1987. *Time Series: Theory and Methods*, Springer-Verlag, Berlin, pp: 320-386.
7. Chatfield, C., 1980. *The Analysis of Time Series. An Introduction*, Chapman and Hall, London.